Analyst

PAPER

View Article Online
View Journal | View Issue

Cite this: *Analyst*, 2026, **151**, 2077

A paper-based immunoassay with signal amplification for the sensitive detection of nucleocapsid protein toward the diagnosis of long COVID

Mônica Duarte da Silva,[a,b] Ruth Speidel, [a] Ayesha Seth, [a] Hianka J. C. Carvalho,[a] Maria A. Miglino[c] and Abraham K. Badu-Tawiah *[a]

Long COVID is characterized by persistent symptoms, including fatigue, cognitive impairment, and respiratory issues, affecting a considerable number of individuals post-infection. The underlying mechanism is not fully understood, but it has been proposed to involve the reactivation of virus, which subsequently induces immune dysregulation. In this proof-of-concept study, we developed a paper-based immunoassay for the detection of nucleocapsid (N) protein, which, due to its stability and low mutation rate, is a valuable biomarker for detecting the presence of residual virus. By utilizing reporter antibodies conjugated to cleavable ionic probes through dendrimer chemistry, we were able to analyze the immunoassay results with ambient mass spectrometry using on-chip paper spray ionization. The used dendrimer enhanced mass spectrometry sensitivity by enabling the attachment of multiple ionic probes to a single reporter antibody. The method presented here achieved a limit of detection of 2.4 pM for N protein detection from paper. Unlike traditional sensitive COVID tests that are only accessible to hospitalized individuals, our paper-based assay has potential to enable long COVID to be detected under resource-limited settings. Our method was applied to analyze 20 human plasma samples, including 10 from individuals with long COVID and 10 from healthy controls with no history of SARS-CoV-2 infection. We observed a significantly higher MS signal—by up to two orders of magnitude—for samples collected from long COVID patients compared to controls. The ability to use the paper device in remote locations was tested by evaluating the stability of the assay, which showed that after 30 days of storage at room temperature, the device retained sufficient analytical performance. Given its robustness, we believe that our platform will be suitable for direct-to-consumer testing, enabling individuals with low viral loads to be screened in a timely fashion.

Received 1st December 2025,
Accepted 12th February 2026

DOI: 10.1039/d5an01267h

rsc.li/analyst

Introduction

The COVID-19 pandemic, caused by the SARS-CoV-2 virus, presented a major challenge to healthcare systems worldwide.[1,2] Traditionally, the acute COVID heals rapidly within four weeks. On the other hand, the post-acute sequalae of SARS-CoV-2 infection, commonly known as long COVID, can present symptoms even 12 weeks after the initial infection.[3] There is a plethora of symptoms for long COVID but there is currently no blood test to diagnose this condition.[4]

The symptoms can be grouped into three categories: (i) detectable damage to organs and tissues, (ii) new chronic illness (*e.g.*, diabetes, blood clots, and fatty liver disease) following the COVID infection, and (iii) long COVID, which involves symptoms in the absence of identifiable conditions. The first two categories (i and ii) can be classified as post-COVID conditions but are not considered as long COVID because they are detectable health challenges with existing treatment. Diagnosing long COVID is challenging because the fundamental source of the strange/mysterious symptoms is not well understood.[5] It has been suggested that the post-exertional malaise, brain fog, and fatigue associated with COVID several months after the initial infection might be caused by reactivation of virus or dysfunction of the immune system due to the presence of virus fragments in the body.[6] These can lead to chronic inflammation that induces autoimmunity where the body attacks itself.

[a]*Department of Chemistry and Biochemistry, The Ohio State University, Columbus, Ohio 43210, USA. E-mail: badu-tawiah.1@osu.edu*
[b]*Department of Surgery, School of Veterinary Medicine and Animal Science, University of Sao Paulo, Sao Paulo 05508-270, Brazil*
[c]*Department of Veterinary Medicine and Animal Science, University of Marilia, Sao Paulo 17525-902, Brazil*

Therefore, a potential blood test targeting specific parts of the SARS-CoV-2 virus could provide a more direct diagnostic approach for long COVID, eliminating the need for patients to undergo multiple hospital visits to rule out conditions with established treatments (*e.g.*, diabetes). Such a test would be particularly relevant given that approximately 6.9% of adults in the United States (around 23 million people in 2022) have experienced long COVID.[7] Of these, 3.4% still report ongoing symptoms, and an estimated 5 million people have been forced out of the workforce due to long COVID, resulting in significant economic losses and an increase in health care costs. Globally, approximately 65 million individuals are expected to have long COVID,[8] with reported prevalence rates of 10–30% among non-hospitalized cases, 50–70% among hospitalized cases[9,10] and 10–12% among vaccinated individuals.[11,12] Interestingly, long COVID disproportionally affects women and people of color.[5] In this context, the development of accessible, affordable, and highly sensitive diagnostic methods is essential. High sensitivity is particularly critical, as the viral fragments potentially responsible for long COVID symptoms often exist at very low concentrations – making the conventional rapid diagnostic test (RDT) unsuitable for reliable detection.

Herein, we present a stable paper-based immunoassay strategy designed to enable early detection of long COVID. This approach will allow patients to collect a finger prick blood sample on an ordinary paper substrate, which can then be analyzed at a central laboratory *via* direct on-chip mass spectrometry (MS). Currently, reverse transcription polymerase chain reaction (RT-PCR) is the gold standard for COVID-19 diagnosis.[13] While highly specific, RT-PCR results can be affected by low viral loads (as is the case for long COVID), sample collection variations, and the complexity of sample processing.[14] These challenges make RT-PCR primarily accessible to hospitalized individuals and difficult to implement in resource-limited settings.[15]

In recent years, MS has emerged as a promising technology for biomarker analysis and molecular diagnostics, offering exceptional sensitivity and the ability to quantify molecules at low concentrations.[16,17] However, applying MS in rapid diagnostics, such as for COVID-19, requires integration with efficient and user-friendly platforms.[18] Thus, immunosensors have been explored as a means of combining MS with simple platforms such as functionalized paper.[19–22]

The nucleocapsid (N) protein is one of the most abundant structural proteins in SARS-CoV-2 infected cells.[23–25] It has been widely studied in diagnostic assays[26–28] in blood and saliva in both symptomatic and asymptomatic cases.[9,10] Additionally, the N protein can persist in the body beyond the acute phase of infection[29] and has a relatively low mutation rate, enhancing its genetic stability and diagnostic utility.[30] Traditional antigen-based tests face challenges in detecting N protein at low viral loads.[31] In contrast, MS-based detection of tagged ions has the capacity to offer a highly sensitive alternative, enabling immunoassay analysis directly from inexpensive paper substrates.

In this proof-of-concept study, we developed a paper-based immunoassay for detecting N protein toward the potential diagnosis of long COVID. The use of cleavable ionic probes allowed on-chip MS analysis of immunoassay results directly from the paper substrate. The MS signal was further amplified *via* a dendrimer-based signal amplification strategy, which allowed a multitude of ionic probes to be attached to a single reporter antibody. As a result, the sensitivity of our paper-based immunoassay was determined to be 2.4 pM for N protein. We also tested the stability of the platform after the assay was complete. Over the 30-day period in which the paper device was stored in ambient air at room temperature, we observed good stability, with a 16.7% reduction in analytical signal compared to the first day. The signal-to-noise (S/N) recorded on the 30th day was >5, which makes it possible to differentiate infected *versus* uninfected samples. We evaluated the clinical capabilities of the method by analyzing 20 human plasma samples among which the 10 samples collected from long COVID patients exhibited an MS signal up to two orders of magnitude higher compared with the 10 control samples.

Experimental section

Chemicals and reagents

Whatman #1 chromatography paper, gel blotting paper, and Grade GB003 sheets (20 × 20 cm) were sourced from Sigma-Aldrich (St Louis, MO, USA). Ultrapure water (18.2 MΩ cm resistivity) was obtained using a Milli-Q Integral system (Merck Millipore, Burlington, MA, USA). Reagents including (3-carboxypropyl)trimethylammonium chloride, 1-ethyl-3-(3-dimethylaminopropyl)carbodiimide hydrochloride, 4-dimethylaminopyridine, acetylcholine, methacholine, phosphate-buffered saline (PBS, pH 7.4), Tris-buffered saline concentrate (10× TBS), and potassium periodate were all purchased from Sigma-Aldrich. Sodium carbonate and sodium bicarbonate were obtained from Fisher Scientific (Hampton, NH, USA), while 4-(2-hydroxyethyl)phenyl isothiocyanate was supplied by Organix Inc. (Woburn, MA, USA). Monoclonal antibodies ABCOV-0401 and ABCOV-0402, both specific to the SARS-CoV-2 nucleoprotein, as well as the AGCOV-0232 antigen corresponding to the viral nucleocapsid protein, were purchased from Arista Biologicals, Inc. (USA).

Mass spectrometry

All mass spectrometry (MS) experiments were performed using an LTQ Velos Pro mass spectrometer (Thermo Fisher Scientific, San Jose, CA, USA). Paper Spray Ionization (PSI) was conducted with a 4.5 kV direct current (DC) spray voltage, using acetonitrile : water (1 : 1, v/v) as the ionization solvent. The solvent was manually applied to the paper substrate to initiate ionization. All spectra were acquired in positive ion mode. Data acquisitions and instrument controls were carried out using XCalibur 2.2 SP1 software (Thermo Fisher Scientific). Tandem MS (MS/MS) with collision-induced dissociation (CID) was employed for structural elucidation of ana-

lytes and identification of diagnostic fragment ions used for quantification. Additional experimental details are provided in the SI.

Clinical samples

Plasma samples were collected from participants recruited at UNIMAR Beneficent Hospital (Marília, São Paulo, Brazil) between January and May 2024. A total of 20 individuals were enrolled in the study: 10 patients diagnosed with long COVID and 10 healthy controls. All participants were between 18 and 60 years of age and provided written informed consent prior to completing a questionnaire and undergoing blood collection. Blood samples were drawn in the morning after an overnight fast of at least 8 hours. Long COVID patients had confirmed SARS-CoV-2 infection by RT-PCR and reported persistent symptoms lasting at least 12 weeks following the acute phase. Control participants were healthy healthcare workers with no history of COVID-19 or other respiratory conditions. Plasma samples were stored at −80 °C until use. This study was conducted in accordance with the ethical guidelines established by the Brazilian National Commission for Research Ethics (CONEP) and was approved by the Research Ethics Committee under registration number CAAE: 31068420.5.0000.5496.

Fabrication and use of 2D microfluidic paper-based devices

In this study, immunoassays were performed using two-dimensional (2D) paper-based analytical devices (μPADs) featuring predefined test zones. These zones were patterned onto cellulose substrates chemically modified with aldehyde functional groups. The wax-patterned 2D μPADs used in this proof-of-concept work were developed and optimized in previous studies by our research group.[20,22,32,33] Briefly, Whatman No. 1 chromatography paper was functionalized in-house with aldehyde groups (Fig. S1). The 2D μPADs were then fabricated *via* solid wax printing, producing circular hydrophilic test zones surrounded by hydrophobic wax barriers (Fig. S2). Detailed protocols for paper modification and the wax patterning used to define the microfluidic regions are provided in the SI. To enable specific detection of SARS-CoV-2 antigens related to long COVID, we used a capture antibody ABCOV-0401 targeting the nucleocapsid protein. This antibody was covalently immobilized onto aldehyde-functionalized paper *via* Schiff base formation, producing a stable and bioactive 2D analytical device (Fig. S3). This functionalization ensured robust antibody binding and high assay performance, as described in detail in the Results and discussion section.

Preparation of ionic probe-conjugated detection antibody

The key innovation of our paper-based immunoassay lies in the in-house synthesis of a cleavable ionic probe and its conjugation to the detection antibody (**dAb**) *via* generation 4 (G4) poly(amidoamine) (PAMAM) dendrimer chemistry, enabling signal amplification for mass spectrometry (MS) analysis.

The pH-sensitive ionic probe, 4-(4-isothiocyanatophenoxy)-*N*,*N*,*N*-trimethyl-4-oxobutaniminium chloride (**ITBA**), was synthesized *via* Steglich esterification,[34] and its structure was confirmed by MS (Fig. S4).

In Fig. 1A we highlight the three essential components of the ionic probe: (1) the pre-charged quaternary ammonium species serves as the mass tag; (2) the ester functional group is the cleavable site, which releases the quaternary ammonium species at pH 11; and (3) the (–NCS) conjugation unit, which enables the whole ionic probe, **ITBA**, to be used for bioconjugation with the G4 PAMAM dendrimer and **dAb**. The synergy among these three components provides a robust system that not only ensures sensitive and specific detection but also improves assay stability, allowing the platform to be stored at room temperature. The bioconjugation process involves three steps, as illustrated in Fig. 1B. The pH-sensitive ionic probe **ITBA** contains an **–NCS** group that reacts with amine groups on the G4 PAMAM dendrimer, forming stable thiourea bonds. The G4 PAMAM dendrimer has 64 amine sites, and the **–NSC** group in **IBTA** allows direct coupling of ionic probes to the dendrimer *via* thiourea chemistry. In the current optimized protocol, we determined that 17 ionic probes are attached to a single G4 PAMAM dendrimer[35] (Fig. 1B(i)). The unreacted amine groups on the dendrimer are treated with glutaraldehyde to introduce aldehyde functionalities (Fig. 1B(ii)). These aldehyde groups enable the next conjugation step by forming Schiff base linkages with lysine residues present in the detection antibody. The detection antibody used (ABCOV-0402, specific to the SARS-CoV-2 nucleocapsid protein) is covalently bound to the dendrimer *via* the newly introduced aldehyde groups (Fig. 1B(iii)). This results in the final bioconjugate structure: an ITBA–dendrimer–detection antibody complex. Detailed protocols for the preparation and purification of the ionic probe–dendrimer–dAb bioconjugate are provided in the SI (Fig. S5).

Results and discussion

Establishment of the sandwich immunoassay on a 2D paper device

A paper-based sandwich immunoassay platform was initially established and tested using a recombinant SARS-CoV-2 nucleocapsid protein to validate the system's functionality. After confirming its performance under controlled conditions, the platform was subsequently applied to human plasma samples from individuals with long COVID, in order to evaluate its ability to discriminate between positive and negative cases.

The assay was conducted within wax-printed hydrophilic test zones, where the capture antibody (cAb) had been previously immobilized. All reagents were manually applied in a stepwise manner. The immobilization procedure began with the dilution of the capture antibody in phosphate-buffered saline (PBS) to a final concentration of 1 mg mL^{-1}. A volume of 4 μL of the diluted cAb was deposited onto the aldehyde-functionalized paper within each test zone. The devices were then incubated for 3 hours at room temperature in a humidity

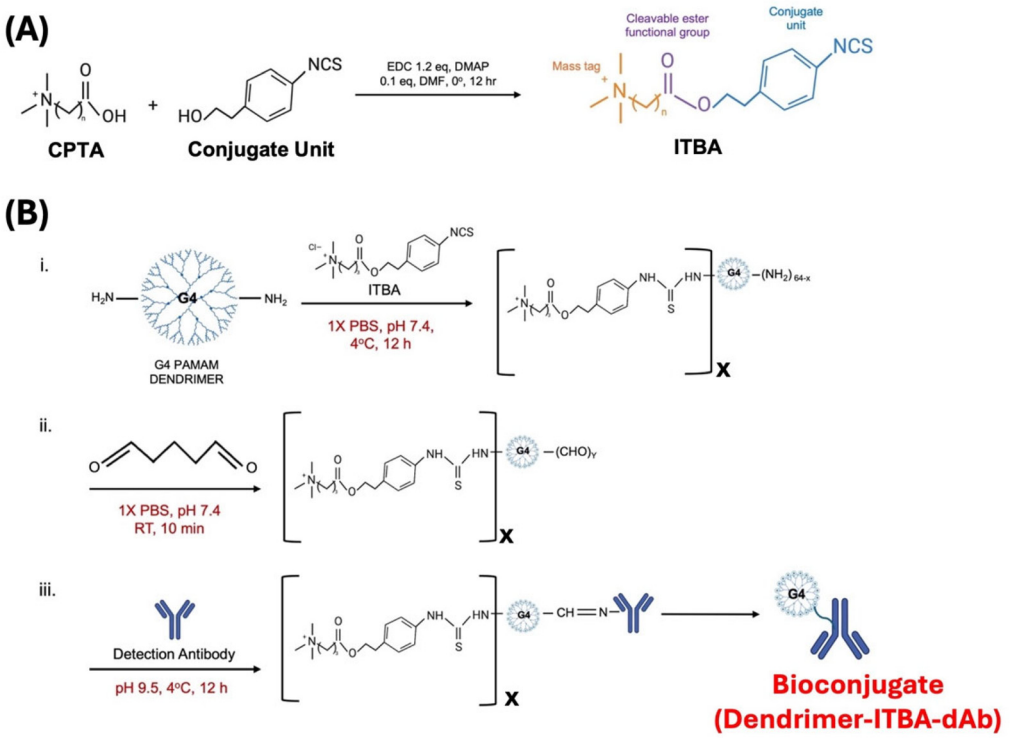

Fig. 1 (A) Synthetic procedure for the pH sensitive ionic probe, 4-(4-isothiocyanatophenoxy)-*N*,*N*,*N*-trimethyl-4-oxobutaniminium chloride (ITBA) *via* Steglich esterification. (B) Bioconjugation process involving (i) the coupling of ITBA to the G4 PAMAM dendrimer, (ii) conversion of excess amine in the dendrimer to aldehyde groups *via* the use of glutaraldehyde, and (iii) application of the detection antibody to produce the final bioconjugate reagent used in the paper-based immunoassay.

chamber to allow covalent immobilization. During this period, the primary amine groups (lysine residues) on the antibody formed Schiff base linkages with the aldehyde groups present on the paper surface, resulting in stable attachment of the antibody. Following immobilization, the test zones were washed twice with 20 μL of 1× PBS to remove unbound antibody.

To block remaining reactive aldehyde sites and prevent nonspecific binding, the zones were incubated with Tris-buffered saline containing 0.05% Tween-20 (**TBS-T**) for 3 hours at room temperature in a humidity chamber. After blocking, the zones were washed again twice with 20 μL of 1× PBS to remove any excess blocking reagent. This blocking step finalized the immobilization process, resulting in the creation of a bioactive paper chip, which was subsequently used in an immunoassay to detect the SARS-CoV-2 N protein. See the SI for details of the full optimization process for producing the bioactive paper chip, which included the optimization of incubation time for immobilization of the capture antibody (Fig. S6), blocking buffer type (Fig. S7) and incubation time (Fig. S8).

The paper-based immunoassay process is illustrated in Fig. 2. Capture of the long COVID biomarker is achieved by adding 20 μL of sample containing the N protein in the test zones created in the bioactive paper chip, followed by incubation for 1 h in a humidity chamber (pipet box filled with water). The test zones were then washed twice with 20 μL of 1× PBS to remove unbound species. As a negative control, some test zones (in a separate bioactive paper chip) were incubated with 20 μL of 1% BSA (bovine serum albumin) in 1× PBS solution to assess the specificity of our assay, which was characterized by the detection of an analytical signal in the absence of the N protein. Next, 5 μL of the detection antibody, specific to the SARS-CoV-2 nucleocapsid protein conjugated to the dendrimer–ionic probe complex, was added to each test zone and incubated for 1 hour at room temperature in a humidity chamber. To complete the immunoassay, the zones were washed twice with 20 μL of PBS-T (0.05% Tween-20), followed by two washes with 20 μL of ultrapure water. After the final wash, the devices were allowed to dry at room temperature and stored under ambient conditions until mass spectrometry analysis *via* on-chip paper spray.

Mass spectrometry analysis *via* on-chip paper spray ionization

To initiate the MS analysis of the completed immunoassay, 8 μL of a cleavage solution containing 2.0 M ammonium hydroxide was applied directly onto the test zone to release the ionic probe. After approximately 20 minutes, the quaternary ammonium compound [(carboxypropyl)trimethylammonium, **CPTA**, MW 146 Da] was liberated (Fig. 3A). For paper spray ionization, the circular wax-printed test zone was carefully cut out and positioned onto a triangular wax-printed paper sub-

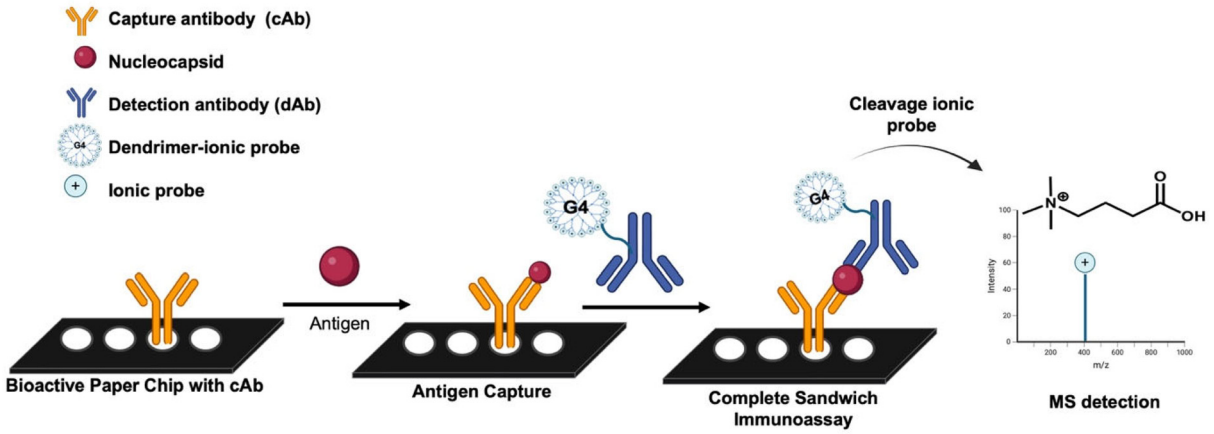

Fig. 2 Sandwich immunoassay workflow. The immunoassay begins by applying the antigen analyte (nucleocapsid protein) onto a bioactive paper chip, to be captured by the immobilized capture antibody. Subsequently, the detection antibody, which has been previously conjugated with a dendrimer and an ionic probe, is added, forming a sandwich complex. After the completion of the sandwich immunoassay, ammonium hydroxide (NH_4OH) is added to cleave the ionic probe, releasing specific ions that are subsequently detected by on-chip paper spray MS.

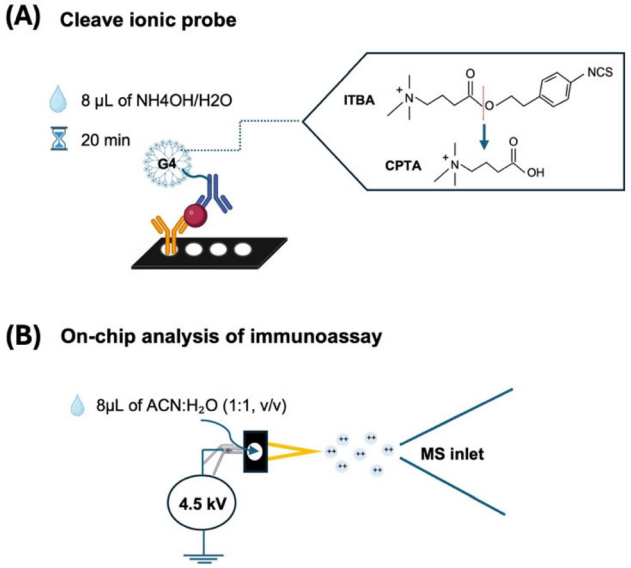

Fig. 3 Workflow summarizing the on-chip PS-MS/MS analysis of a paper-based sandwich immunoassay for long COVID detection. (A) A basic NH_4OH/H_2O solution (8 µL, pH ≈ 11) is applied to the test zones to cleave the ionic probes from the immunocomplex after 20 minutes of incubation. (B) The test zone is cut and mounted on a conductive triangular support. An alligator clip connects the paper to a 4.5 kV power supply and aligns it with the mass spectrometer (MS) inlet. A solvent mixture (8 µL of ACN : H_2O, 1 : 1, v/v) is added to initiate paper spray ionization, directing the cleaved probes into the MS for detection.

strate (dimensions: 9 mm base, 16 mm height, and a 33° tip angle) specifically designed for on-chip MS analysis. The two pieces of paper were clamped together with an alligator clip and oriented in front of the mass spectrometer inlet. A spray solvent composed of acetonitrile and water (1 : 1, v/v) was applied to the assembly. The released ionic probe was[20] transferred (with 98% efficiency)[20] from the circular zone to the triangular substrate (Fig. 3B). Then, a high voltage of 4.5 kV was applied to the wetted paper, inducing electrospray at the tip of the triangular region and generating charged microdroplets that carried the cleaved CPTA ions toward the mass spectrometer. To enhance detection specificity, the signal corresponding to the CPTA quaternary ammonium species was analyzed by tandem MS using collision-induced dissociation (CID-MS/MS). This approach enabled the identification of a characteristic fragment ion at *m*/*z* 87, confirming the presence of an ionic probe. See the SI for details of PS-MS analysis (Fig. S9).

Fig. 4A shows a representative positive-ion CID-MS/MS spectrum of the probe (1 µM), highlighting the expected diagnostic fragment ions. A constant amount of internal standard, (carboxymethyl)trimethylammonium chloride (CMTA; MW 118 Da), was included in all experiments to normalize potential variability across different samples.

The internal standard, which has a similar chemical structure to the cleaved quaternary ammonium compound, generates a characteristic fragment ion at *m*/*z* 59 upon CID MS/MS fragmentation, as demonstrated in Fig. 4B for 10 µM CPTA. The analytical measurement for each sample is obtained by calculating the ratio of the quaternary ammonium species signal at *m*/*z* 87 to the internal standard signal at *m*/*z* 59. This ratio serves as the quantitative indicator in the immunoassay performed on the test zones.

All optimization steps were initially performed using the purchased recombinant nucleocapsid protein. The parameters optimized included the duration of the covalent immobilization process for the capture antibody, the selection of blocking buffer type and its incubation time, and the concentration of the detection antibody conjugate (see the SI for details of the full optimization process). After establishing the optimal conditions with the recombinant protein, these parameters were applied to analyze clinical plasma samples.

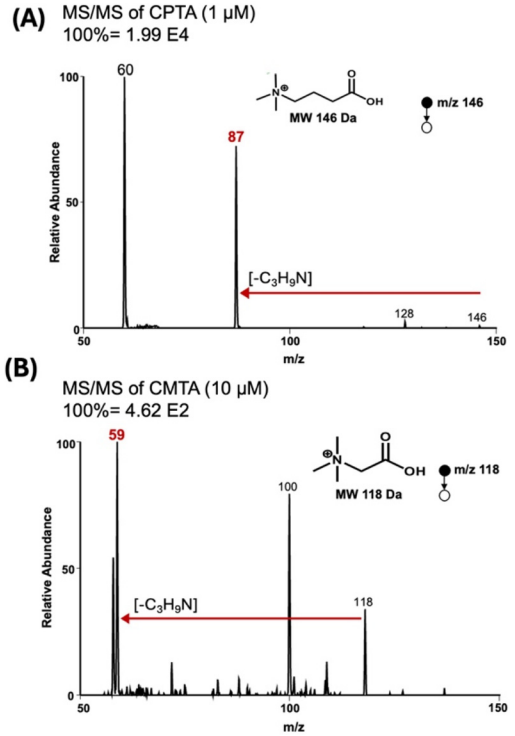

Fig. 4 Positive-ion mode paper spray MS/MS analysis of (A) released quaternary ammonium species, (carboxypropyl)trimethylammonium (CPTA) at *m*/*z* 146 after base hydrolysis (pH 11) of the purified bioconjugate, which gives a diagnostic fragment ion at *m*/*z* 87 and (B) (carboxymethyl)trimethylammonium chloride (CMTA) at *m*/*z* 118 used as an internal standard, showing a fragment ion at *m*/*z* 59.

Considering that the immunoassay for analyte detection begins once the sample is applied to the bioactive paper chip, the optimized 1 h incubation time represents the total assay duration in the final version of the platform. While the current 2D μPAD implementation involves manual steps, the envisioned 3D μPAD will store all reagents within the device, enabling a fully automated and user-friendly immunoassay.[33]

The SARS-CoV-2 nucleocapsid (N) protein stands out as one of the most abundant, conserved, and immunogenic structural proteins of the virus,[36] making it a highly attractive target for diagnostic applications. In contrast to the spike (S) glycoprotein, which is subject to frequent mutations that may compromise assay sensitivity, the N protein exhibits greater genetic stability across emerging variants.[37] This characteristic ensures reliable detection even as the virus evolves. Additionally, the N protein is expressed early during infection, allowing for prompt identification of cases, which is critical for timely intervention measures such as isolation and contact tracing.[38] Compared to RNA-based detection methods, which are susceptible to false negatives due to RNA degradation or low viral load, the detection of the N protein offers increased diagnostic robustness. Its high degree of conservation among different coronavirus strains further extends its utility beyond COVID-19, positioning the N protein as a broadly applicable biomarker for coronavirus surveillance.[39,40] These features collectively highlight the value of targeting the N protein in diagnostic strategies, especially in the context of long COVID and future emerging pathogens.

Calibration curve and sensitivity assessment

The sensitivity of our paper-based immunoassay for the SARS-CoV-2 nucleocapsid (N) protein was evaluated using internal standard calibration. Standard solutions of recombinant N protein were prepared in 1× PBS at concentrations ranging from 2 to 200 pM. Each concentration was analyzed following the immunoassay procedure described in Fig. 2, and the results were evaluated by on-chip paper spray mass spectrometry after cleavage of the ionic probe. The MS/MS signal corresponding to the cleaved probe (CPTA, *m*/*z* 87) was compared to that of the internal standard, (carboxymethyl)trimethylammonium (CMTA, *m*/*z* 59). A representative MS/MS spectrum from the assay using 20 pM N protein is shown in Fig. 5A, demonstrating a strong diagnostic signal at *m*/*z* 87. In contrast, negative control samples prepared with 1% BSA and no N protein also exhibited a peak at *m*/*z* 87, but with a significantly lower intensity (Fig. 5B), indicating minimal nonspecific binding in our platform. MS/MS data collected across the full concentration range are shown in Fig. 5C, displaying a sigmoidal response curve on a logarithmic scale, as typically expected for immunoassays. The linear dynamic range, presented in Fig. 5D, showed excellent linearity ($R \geq 0.99$) between 5 and 40 pM. Based on this calibration, the limit of detection (LOD) was determined to be 2.4 pM (161.2 pg mL^{-1}), and the limit of quantification (LOQ) was 7.9 pM (535.2 pg mL^{-1}).

Our paper-based immunoassay with MS signal transduction demonstrated excellent performance, exhibiting a highly linear regression coefficient (R^2) > 0.99. The observed LOD and LOQ values are among the lowest reported for mass spectrometry-based methods detecting viral nucleocapsid, thus marking a significant advancement in potential early detection of SARS-CoV-2 infections. The low LOD observed in this study underscores the system's superior sensitivity compared to traditional diagnostic methods. While PCR offers high sensitivity, the extensive sample preparation requires the patient to be at the hospital to gain access to the test. The paper-based assay presented here with analytical signal amplification (not analyte amplification) has potential to offer on-demand testing to diagnose long COVID from whole blood without any sample pre-treatment. For example, the sensitivity of our current assay falls within the clinically relevant range of nucleocapsid levels in individuals infected with SARS-CoV-2, which have been reported to vary from 1 pg mL^{-1} to over 10 000 pg mL^{-1}.[9,23] This confirms the method's suitability for detecting infections, including those in individuals with low viral loads, thus enabling more effective and timely screening. The system's ability to detect viral nucleocapsid at such a low concentration of 2.4 pM affirms its potential for early-stage detection and monitoring of COVID.

Clinical application

Following the successful optimization and analytical validation of the assay using recombinant N protein, we next applied the

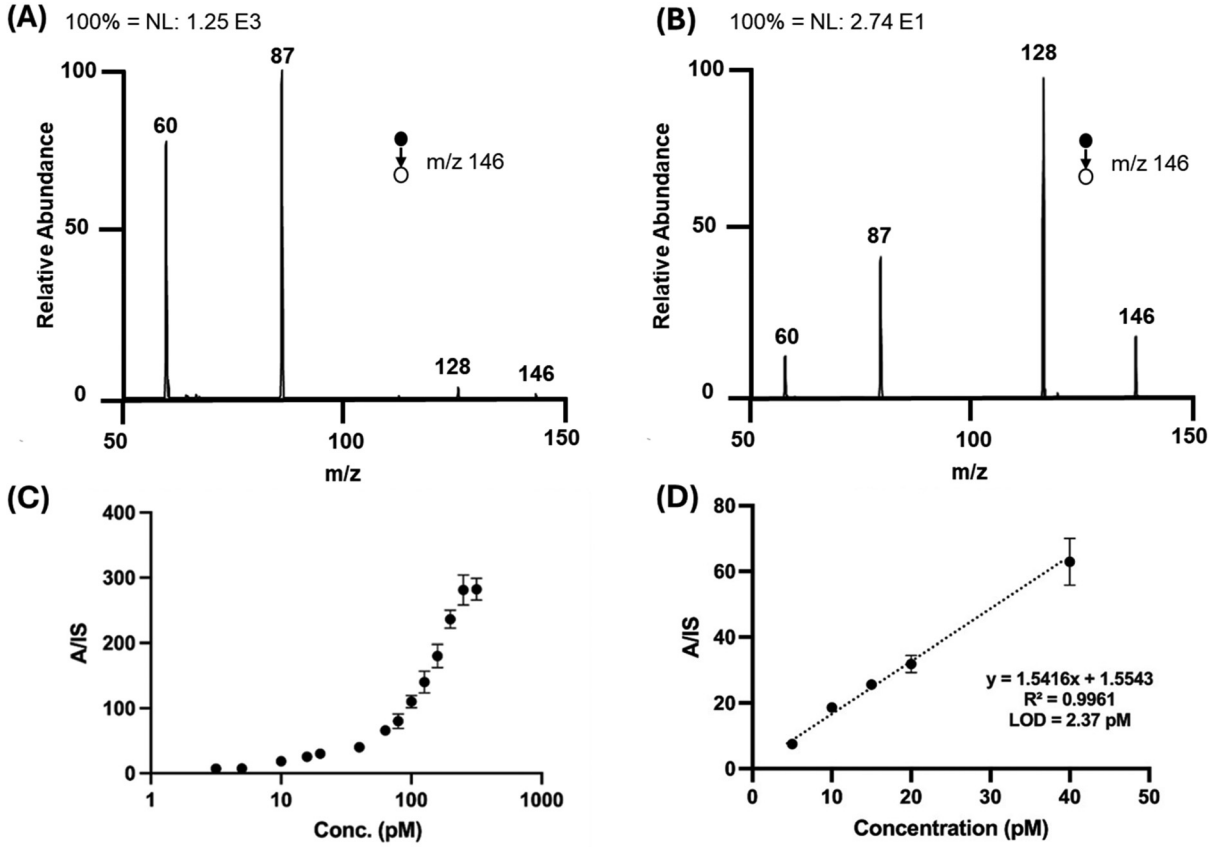

Fig. 5 On-chip paper spray PS-MS/MS analysis of the completed paper-based immunoassay. (A) Typical MS/MS spectrum from the analysis of 20 pM N protein in our paper-based immunoassay. (B) MS/MS spectrum obtained from a negative/blank sample in the immunoassay. (C) Log-scale calibration curve depicting the full concentration range (2–200 pM) derived from comparing the MS/MS signal of the assay (*m*/*z* 87) to that of internal standard (*m*/*z* 59). (D) Linear range of the calibration curve, used to determine the LOD and LOQ. The LOD and LOQ were calculated as follows: LOD = 3 × SD (blank)/slope; LOQ = 10 × SD (blank)/slope. SD = standard deviation.

platform to analyze clinical plasma samples. The plasma samples were collected from 20 individuals: 10 patients with clinically confirmed long COVID and 10 SARS-CoV-2-negative controls with no documented history of infection. The samples were diluted 1 : 80 (vol/vol) in a negative commercial plasma, and then 20 μL of the diluted plasma was applied to the bioactive paper chip and processed according to the optimized immunoassay protocol. Detection was based on the MS/MS signal of the cleaved ionic probe (CPTA, *m*/*z* 87), which reflects the presence of the SARS-CoV-2 nucleocapsid antigen in these long COVID samples.

Representative MS/MS spectra derived from analyzing a plasma sample from a long COVID patient and a negative control are shown in Fig. 6A and B, respectively. As expected, the signal intensity at *m*/*z* 87 was elevated in the positive sample, while the negative sample exhibited only minimal background response. Fig. 6C summarizes the comparative analysis *via* a box and whisker plot, clearly illustrating a significant difference for the 10 long COVID samples compared with the 10 control patients ($p < 0.01$). The elevated signal in the long COVID group provides molecular evidence supporting the persistence of SARS-CoV-2 nucleocapsid protein beyond the acute infection phase. Despite the relatively small sample size, the observed distinction between the two groups was consistently replicated within the groups, underscoring the minimal matrix effects, high reproducibility, and analytical power of the platform. The fact that no overlap in analytical signal is observed (Fig. 6C) between the positive and negative samples demonstrates the high accuracy of our paper-based immunoassay platform in predicting the state of the disease as indicated by PCR. Our ability to detect residual viral antigen in post-acute samples suggests that this assay may serve as a useful tool to explore the pathophysiological underpinnings of long COVID. The detection of nucleocapsid protein in convalescent individuals supports the hypothesis that persistent antigenemia may contribute to chronic immune activation or prolonged symptomatology.

These results extend the potential clinical utility of paper-based MS immunoassays beyond acute diagnostics, offering a foundation for the future development of direct-to-consumer (DTC) testing for monitoring long-term infection sequelae. Our approach is technologically flexible, allowing the process to be readily refined as new long COVID biomarkers become viable. Aside from DTC testing, we envision that the method

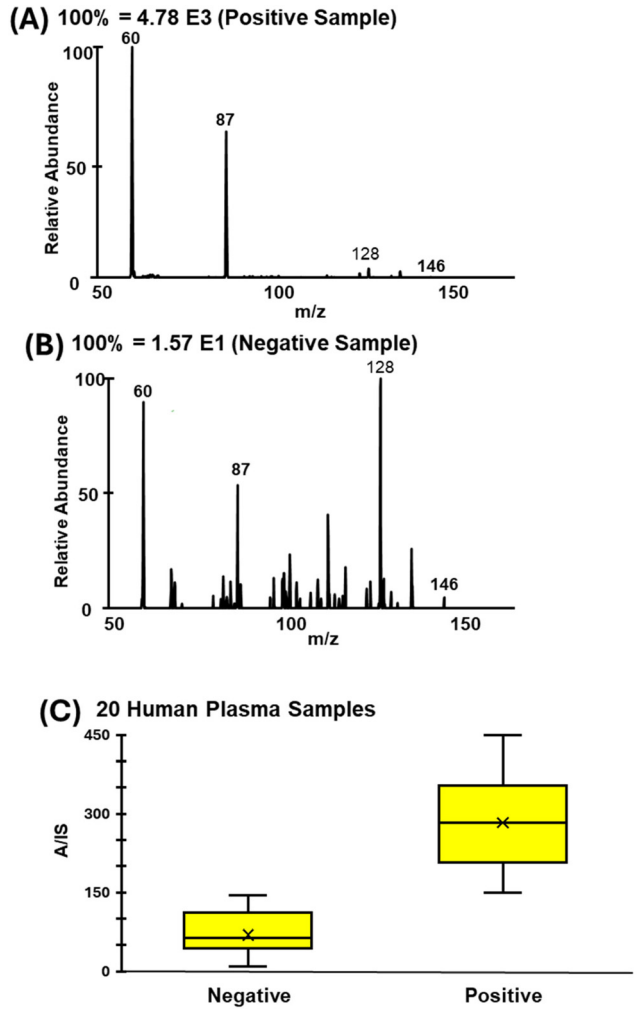

Fig. 6 Representative results from the paper-based immunoassay applied to clinical plasma samples. (A) MS/MS spectrum of a positive plasma sample from a long COVID patient showing a strong signal at *m*/*z* 87, corresponding to the cleaved ionic probe (CPTA). (B) MS/MS spectrum from a SARS-CoV-2-negative control sample showing a substantially lower signal at *m*/*z* 87. (C) Boxplot comparing the CPTA signal intensity (*m*/*z* 87) between long COVID (n = 10) and negative control samples (n = 10). A significant difference was observed between the two groups ($p < 0.01$), demonstrating the assay's ability to discriminate based on the presence of residual nucleocapsid protein.

will also be applicable for point-of-care (POC) testing for hospitalized patients, where long COVID can be differentiated from other conditions with existing treatment.

Device stability

To enable on-demand DTC testing, where samples are collected and analyzed at two different places, it is necessary for the assay to be stable to provide actionable results even weeks after the test is completed. Here, we performed two stability studies: one evaluating the stability of the capture antibody, which shows the shelf-life of the bioactive paper chip, and a second evaluating the stability of the whole immunoassay complex in the paper substrate after the assay is completed.

For shelf-life stability studies, the capture antibody was immobilized in the 2D wax-printed paper substrate, blocked, and stored in ambient air at room temperature. On the day of the analysis, a 100 pM solution of N protein was applied to the bioactive paper chip followed by the addition of ionic probe–dendrimer–dAb bioconjugate to complete the assay. Then, the completed paper-based immunoassay was analyzed immediately. This process was repeated for paper chips stored in ambient air for up to 30 days, and the assay was performed 0, 5, 8, 15, 25 and 30 days after storage. The results of this stability study are provided in Fig. 7A, which shows a relatively stable signal over the 30-day storage period. There is a signal drop of about 12% compared with the onset of the study but the positive signal detected is significantly higher than non-specific background noise. Instead of storing at room temperature, the shelf-life of the capture antibody can be further extended by storing it in a refrigerator until use.

The second stability study evaluated the feasibility of on-demand testing, where completed assays could be mailed in ordinary envelopes to a centralized facility for analysis. In this experiment, paper-based immunoassays were completed simultaneously and stored in a drawer under ambient conditions for up to 30 days. At specific time points (0, 5, 8, 15, 20 and 25 days), NH_4OH solution was applied to the paper substrate to cleave the bound ionic probe, releasing CPTA for subsequent on-chip paper spray MS/MS analysis. The results are presented in Fig. 7B. As can be observed, the signal from positive samples

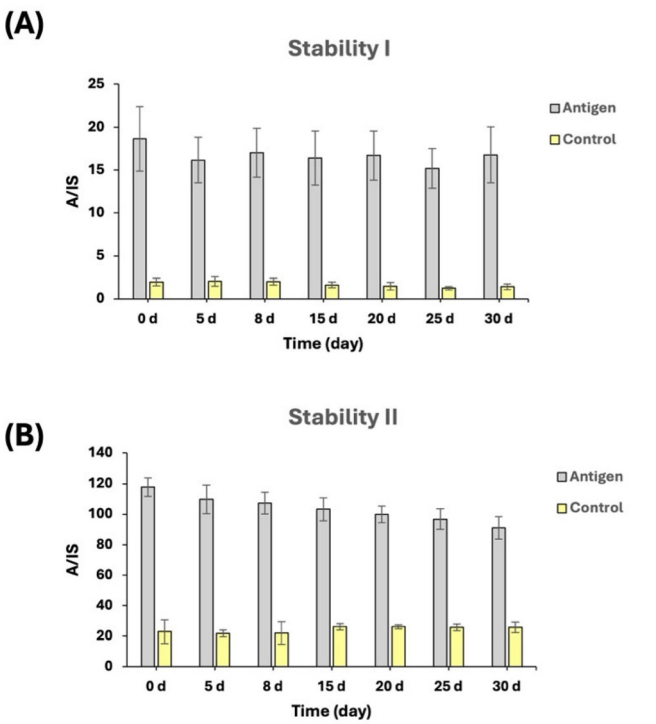

Fig. 7 Study on the stability of paper chips stored at room temperature. (A) Stability I. The capture antibody was stored on the paper at room temperature. The assay was performed and analyzed on the day of testing. (B) Stability II. Investigation of test stability after the addition of the detection antibody (dAb) and completion of the immunoassay.

remained relatively stable throughout the storage period. However, by day 30, a signal reduction of approximately 16.7% was observed compared to day 1, when the assay was analyzed 24 hours after completion. These findings underscore the practicality of decoupling sample collection from immediate analysis, offering significant operational flexibility. This approach allows healthcare professionals to collect multiple samples without requiring on-site processing, making the method more adaptable, cost-effective, and highly sensitive. Moreover, the ability to maintain signal stability over an extended period reinforces the feasibility of decentralized sample collection followed by centralized high-precision analysis.

The current results are consistent with previous studies that demonstrated the effectiveness of functionalized paper in rapid immunoassays,[20,32] highlighting its stability for up to 30 days when stored at ambient temperature. The main advantage of our system over conventional methods, such as ELISA and PCR, lies in the lack of sample preparation. When fully developed, our method will utilize a 3D microfluidic paper-based analytical device (μPAD), in which all the reagents needed for the assay can be stored within the device. In this case, only two steps are required to complete the assay: application of whole blood and a washing step.[33] The combination of a plasma separation membrane and a paper substrate allows in-chip removal of red blood cells, and the resulting plasma subsequently moves *in situ* into the 3D μPAD platform *via* capillary action without any active pumping, all facilitating the potential use of our method in resource-limited settings. Such capabilities highlight the practical and commercial feasibility of the method, which can be easily adapted for various field applications, including large-scale testing during an outbreak, due to its wide accessibility through remote sample collection followed by analysis of the collected samples anywhere with an existing mass spectrometer, especially when combined with a portable mass spectrometer. We are also able to eliminate cold-chain logistics during sample transportation due to room temperature stability.

Beyond infectious disease diagnostics, this platform has potential for broader applications, including early cancer biomarker detection, therapeutic drug monitoring, metabolic disorder screening, and even environmental surveillance through the highly sensitivity wax-printed paper spray method for detecting metabolites.[41] Its adaptability could also support personalized medicine approaches, where patient-specific biomarker profiles guide treatment strategies in real time. Additionally, the technology could be leveraged in veterinary medicine and agricultural pathogen monitoring, expanding its impact beyond human healthcare. Future advancements may allow for multiplexed detection of multiple analytes within a single test, thereby increasing efficiency and further enhancing the platform's applicability in diverse settings.

Conclusion

In summary, we developed a highly sensitive and stable paper-based immunoassay for N protein detection, which enables direct mass spectrometric analysis from a paper substrate. The combination of cleavable ionic probes and a dendrimer-based amplification strategy, which allows multiple probes to be linked to a single reporter antibody, resulted in a detection limit of 2.4 pM. The platform also exhibited good analytical stability, with only a 16.7% reduction in signal after 30 days of storage under ambient conditions. These findings underscore the potential of this system for long COVID diagnostics in both direct-to-consumer and point-of-care settings. To evaluate this possibility, we applied the assay to analyze clinical plasma samples, with 10 long COVID samples showing consistent MS signals compared with samples from 10 uninfected individuals. This result is important because the detection of residual nucleocapsid antigen in convalescent plasma samples supports the hypothesis of persistent antigenemia and chronic immune activation in long COVID.

Although clinical validation and integration into routine diagnostic workflows are necessary for large-scale adoption, the platform's robustness, flexibility in incorporating emerging biomarkers, and suitability for decentralized sample collection support its broader applicability. While the study presents a promising and versatile diagnostic tool that may advance the detection and monitoring of long COVID and other chronic viral conditions, some improvements are needed to achieve this objective. For example, multiplexed detection with other viral biomarkers must be explored to improve the accuracy of diagnostic outcomes. The automated process in the form of 3D μPAD must also be established to reduce the current 2 h assay time and to make it more user friendly. Overall, the ability of the platform to provide quantitative results with high accuracy positions it as a valuable tool for epidemiological studies and real-time monitoring of viral outbreaks, aiding in public health decision-making and response strategies.

Author contributions

The manuscript was written with contributions from all authors, who have all reviewed and approved the final version.

Conflicts of interest

There are no conflicts to declare.

Data availability

The data that support the findings of this study are available in the supplementary information (SI). Supplementary information: preparation of aldehyde-functionalized paper for covalent immobilization of amine-containing biomolecules, wax printing for hydrophobic barrier formation, fabrication of bioactive paper chips, synthesis of ionic probes, preparation of the detection antibody conjugated with the probe, optimization of immunoassay parameters including capture antibody concentration, selection of the blocking buffer type, determi-

nation of the optimal blocking time, and PS-MS analysis for detection and quantification (file type: PDF). See DOI: https://doi.org/10.1039/d5an01267h.

Acknowledgements

This study was funded by the National Institutes of Health (R01AI143809-01), startup funds provided by the Ohio State University, and the Brazilian National Council for Scientific and Technological Development (CNPq, grant no. 200177/2022-2).

References

1 I. F. Miller, A. D. Becker, B. T. Grenfell and C. J. E. Metcalf, Disease and healthcare burden of COVID-19 in the United States, *Nat. Med.*, 2020, **26**(8), 1212–1217, DOI: 10.1038/s41591-020-0952-y.

2 M. L. Metersky, D. Rodrick, S. Y. Ho, D. Galusha, A. Timashenka, E. N. Grace, D. Marshall, S. Eckenrode and H. M. Krumholz, Hospital COVID-19 burden and adverse event rates, *JAMA Netw. Open*, 2024, **7**(11), e2442936, DOI: 10.1001/JAMANETWORKOPEN.2024.42936.

3 M. D. da Silva, T. S. da Silva, C. G. Mendes, M. C. M. Valbão, A. K. Badu-Tawiah, L. F. Laurindo, S. M. Barbalho, R. Direito and M. A. Miglino, Advances in understanding long COVID: Pathophysiological mechanisms and the role of omics technologies in biomarker identification, *Mol. Diagn. Ther.*, 2025, **2025**, 1–20, DOI: 10.1007/S40291-025-00792-8.

4 H. E. Davis, L. McCorkell, J. M. Vogel, E. J. Topol and C. O. V. I. D. Long, Major findings, mechanisms and recommendations, *Nat. Rev. Microbiol.*, 2023, **21**(3), 133–146, DOI: 10.1038/s41579-022-00846-2.

5 M. Verduzco-Gutierrez, T. K. Fleming and A. M. Azola, Considerations for long COVID rehabilitation in women, *Phys. Med. Rehabil. Clin. N. Am.*, 2025, **36**(2), 371–387, DOI: 10.1016/J.PMR.2024.11.009.

6 Y. Zhang, V. Bharathi, T. Dokoshi, J. d. Anda, L. T. Ursery, N. N. Kulkarni, Y. Nakamura, J. Chen, E. W. C. Luo, L. Wang, H. Xu, A. Coady, R. Zurich, M. W. Lee, H. K. Lee, L. C. Chan, T. Matsui, A. A. Schepmoes, M. S. Lipton, R. Zhao, J. N. Adkins, G. C. Clair, L. R. Thurlow, J. C. Schisler, M. C. Wolfgang, R. S. Hagan, M. R. Yeaman, T. M. Weiss, X. Chen, M. M. H. Li, V. Nizet, S. Antoniak, N. Mackman, R. L. Gallo and G. C. L. Wong, Viral afterlife: SARS-CoV-2 as a reservoir of immunomimetic peptides that reassemble into proinflammatory supramolecular complexes, *Proc. Natl. Acad. Sci. U. S. A.*, 2024, **121**(6), e2300644120, DOI: 10.1073/PNAS.2300644120/SUPPL_FILE/PNAS.2300644120.SAPP.PDF.

7 D. Adjaye-Gbewonyo, A. Vahratian, C. G. Perrine and J. Bertolli, *Key findings data from the National Health interview survey: what percentage of adults ever had long COVID or currently have long COVID, and did it differ by sex?*, 2022. https://www.cdc.gov/nchs/products/index.htm.

8 A. V. Ballering, S. K. R. van Zon, T. C. olde Hartman and J. G. M. Rosmalen, Persistence of somatic symptoms after COVID-19 in the Netherlands: An observational cohort study, *Lancet*, 2022, **400**(10350), 452–461, DOI: 10.1016/S0140-6736(22)01214-4.

9 D. Shan, J. M. Johnson, S. C. Fernandes, M. Mendes, H. Suib, M. Holdridge, E. M. Burke, K. Beauregard, Y. Zhang, M. Cleary, S. Xu, X. Yao, P. Patel, T. Plavina, D. Wilson, L. Chang, K. M. Kaiser, J. Natterman, S. V. Schmidt, E. Latz, K. Hrusovsky, D. Mattoon and A. J. Ball, SARS-Coronavirus-2 nucleocapsid protein measured in blood using a Simoa ultra-sensitive immunoassay differentiates COVID-19 infection with high clinical sensitivity, *medRxiv*, 2020, preprint, medRxiv:2020.08.14.20175356. DOI: 10.1101/2020.08.14.20175356.

10 D. Shan, J. M. Johnson, S. C. Fernandes, H. Suib, S. Hwang, D. Wuelfing, M. Mendes, M. Holdridge, E. M. Burke, K. Beauregard, Y. Zhang, M. Cleary, S. Xu, X. Yao, P. P. Patel, T. Plavina, D. H. Wilson, L. Chang, K. M. Kaiser, J. Nattermann, S. V. Schmidt, E. Latz, K. Hrusovsky, D. Mattoon and A. J. Ball, N-Protein presents early in blood, dried blood and saliva during asymptomatic and symptomatic SARS-CoV-2 Infection, *Nat. Commun.*, 2021, **12**(1), 1–8, DOI: 10.1038/s41467-021-22072-9.

11 Z. Al-Aly, B. Bowe and Y. Xie, Long COVID after breakthrough SARS-CoV-2 infection, *Nat. Med.*, 2022, **28**(7), 1461–1467, DOI: 10.1038/s41591-022-01840-0.

12 D. Ayoubkhani, M. L. Bosworth, S. King, K. B. Pouwels, M. Glickman, V. Nafilyan, F. Zaccardi and K. Khunti, Risk of long Covid in people infected with SARS-CoV-2 after two doses of a COVID-19 vaccine: Community-based, matched cohort study, *medRxiv*, 2022, preprint, medRxiv:2022.02.23.22271388. DOI: 10.1101/2022.02.23.22271388.

13 M. Dramé, M. T. Teguo, E. Proye, F. Hequet, M. Hentzien, L. Kanagaratnam and L. Godaert, Should RT–PCR be considered a gold standard in the diagnosis of COVID-19?, *J. Med. Virol.*, 2020, **92**(11), 2312, DOI: 10.1002/JMV.25996.

14 G. Lippi, A. M. Simundic and M. Plebani, Potential preanalytical and analytical vulnerabilities in the laboratory diagnosis of coronavirus disease 2019 (COVID-19), *Clin. Chem. Lab. Med.*, 2020, **58**(7), 1070–1076, DOI: 10.1515/CCLM-2020-0285/MACHINEREADABLECITATION/RIS.

15 B. Udugama, P. Kadhiresan, H. N. Kozlowski, A. Malekjahani, M. Osborne, V. Y. C. Li, H. Chen, S. Mubareka, J. B. Gubbay and W. C. W. Chan, Diagnosing COVID-19: The disease and tools for detection, *ACS Nano*, 2020, **14**(4), 3822–3835, DOI: 10.1021/ACSNANO.0C02624/ASSET/IMAGES/LARGE/NN0C02624_0004.JPEG.

16 H. Y. Lee, E. G. Kim, H. R. Jung, J. W. Jung, H. B. Kim, J. W. Cho, K. M. Kim and E. C. Yi, Refinements of LC-MS/MS spectral counting statistics improve quantification of low abundance proteins, *Sci. Rep.*, 2019, **9**(1), 1–10, DOI: 10.1038/s41598-019-49665-1.

17 S. Rankin-Turner, P. Sears, L. M. Heaney, S. Rankin-Tuner and W. H. Feinstone, Applications of ambient ionization mass spectrometry in 2022, An Annual Review, *Anal. Sci. Adv.*, 2023, **4**(5–6), 133–153, DOI: 10.1002/ANSA.202300004.

18 D. Silva, I. W. Nayek, S. Singh, V. Reddy, J. Granger, J. K. Verbeck and G. F, Paper spray mass spectrometry utilizing Teslin® substrate for rapid detection of lipid metabolite changes during COVID-19 infection, *Analyst*, 2020, **145**(17), 5725–5732, DOI: 10.1039/D0AN01074J.

19 J. Sun, J. H. Song, M. K. Danielson, N. D. Colley, A. Thomas, D. Hambly, J. C. Barnes and M. L. Gross, Development of a high-throughput mass spectrometry-based SARS-CoV-2 immunoassay, *Anal. Chem.*, 2024, **96**(1), 12–17, DOI: 10.1021/ACS.ANALCHEM.3C02421/ASSET/IMAGES/LARGE/AC3C02421_0007.JPEG.

20 S. Lee, D. S. Kulyk, S. O. Afriyie, K. Badu and A. K. Badu-Tawiah, Malaria diagnosis using paper-based immunoassay for clinical blood sampling and analysis by a miniature mass spectrometer, *Anal. Chem.*, 2022, **94**(41), 14377–14384, DOI: 10.1021/ACS.ANALCHEM.2C03105/SUPPL_FILE/AC2C03105_SI_001.PDF.

21 S. Chen, Q. Wan and A. K. Badu-Tawiah, Mass spectrometry for paper-based immunoassays: Toward on-demand diagnosis, *J. Am. Chem. Soc.*, 2016, **138**(20), 6356–6359, DOI: 10.1021/JACS.6B02232/SUPPL_FILE/JA6B02232_SI_001.PDF.

22 S. Jackson, S. Lee and A. K. Badu-Tawiah, Automated immunoassay performed on a 3D microfluidic paper-based device for malaria detection by ambient mass spectrometry, *Anal. Chem.*, 2022, **94**(12), 5132–5139, DOI: 10.1021/ACS.ANALCHEM.1C05530/SUPPL_FILE/AC1C05530_SI_001.PDF.

23 T. Li, L. Wang, H. Wang, X. Li, S. Zhang, Y. Xu and W. Wei, Serum SARS-COV-2 nucleocapsid protein: A sensitivity and specificity early diagnostic marker for SARS-COV-2 infection, *Front. Cell. Infect. Microbiol.*, 2020, **10**, 569444, DOI: 10.3389/FCIMB.2020.00470/BIBTEX.

24 Z. Bai, Y. Cao, W. Liu and J. Li, The SARS-CoV-2 nucleocapsid protein and its role in viral structure, biological functions, and a potential target for drug or vaccine mitigation, *Viruses*, 2021, **13**(6), 1115, DOI: 10.3390/V13061115.

25 T. Gao, Y. Gao, X. Liu, Z. Nie, H. Sun, K. Lin, H. Peng and S. Wang, Identification and functional analysis of the SARS-COV-2 nucleocapsid protein, *BMC Microbiol.*, 2021, **21**(1), 1–10, DOI: 10.1186/S12866-021-02107-3/TABLES/4.

26 Y. Zhang, C. M. Ong, C. Yun, W. Mo, J. D. Whitman, K. L. Lynch and A. H. B. Wu, Diagnostic value of nucleocapsid protein in blood for SARS-CoV-2 infection, *Clin. Chem.*, 2021, **68**(1), 240–248, DOI: 10.1093/CLINCHEM/HVAB148.

27 D. Wang, Y. Shen, J. Wu, Y. Li, K. Ma, G. Jiang, X. Li, H. Qin, K. Chen, M. Wang, Z. Wu and M. Guan, in *Plasma Nucleocapsid Protein: A Potential Beacon for COVID-19 Severity Prediction and Prognostic Insight in Severe Patients with Comorbidities*, 2024. DOI: 10.21203/RS.3.RS-4531889/V1.

28 W. Wu, Y. Cheng, H. Zhou, C. Sun and S. Zhang, The SARS-CoV-2 nucleocapsid protein: Its role in the viral life cycle, structure and functions, and use as a potential target in the development of vaccines and diagnostics, *Virol. J.*, 2023, **20**(1), 1–16, DOI: 10.1186/S12985-023-01968-6.

29 C. C. L. Cheung, D. Goh, X. Lim, T. Z. Tien, J. C. T. Lim, J. N. Lee, B. Tan, Z. E. A. Tay, W. Y. Wan, E. X. Chen, S. N. Nerurkar, S. Loong, P. C. Cheow, C. Y. Chan, Y. X. Koh, T. T. Tan, S. Kalimuddin, W. M. D. Tai, J. L. Ng, J. G. H. Low, J. Yeong and K. H. Lim, Residual SARS-CoV-2 viral antigens detected in GI and hepatic tissues from five recovered patients with COVID-19, *Gut*, 2022, **71**(1), 226–229, DOI: 10.1136/GUTJNL-2021-324280.

30 N. Muradyan, V. Arakelov, A. Sargsyan, A. Paronyan, G. Arakelov and K. Nazaryan, Impact of mutations on the stability of SARS-CoV-2 nucleocapsid protein structure, *Sci. Rep.*, 2024, **14**(1), 1–11, DOI: 10.1038/s41598-024-55157-8.

31 F. Maghsood, A. Ghorbani, H. Yadegari, F. Golsaz-Shirazi, M. M. Amiri and F. Shokri, SARS-CoV-2 nucleocapsid: Biological functions and implication for disease diagnosis and vaccine design, *Rev. Med. Virol.*, 2023, **33**(3), e2431, DOI: 10.1002/RMV.2431.

32 H. J. C. de Carvalho, A. Seth, R. Speidel, A. L. Abreu-Silva, H. M. de Andrade, M. A. Miglino and A. K. Badu-Tawiah, A 2D microfluidic paper-based analytical device for diagnosis of canine visceral Leishmaniasis via mass spectrometry-based immunoassay, *Anal. Chem.*, 2025, **97**(13), 7089–7097, DOI: 10.1021/ACS.ANALCHEM.4C05962/SUPPL_FILE/AC4C05962_SI_001.PDF.

33 A. Seth, S. Lee, G. Muralikrishnan, E. Garcia, J. Odei, A. H. Mutala, K. Badu and A. K. Badu-Tawiah, Diagnosis on-demand: Field evaluation of microfluidic paper device for the detection of asymptomatic malaria, *Anal. Chem.*, 2025, **97**(22), 11787–11797, DOI: 10.1021/acs.analchem.5c01324.

34 B. Neises and W. Steglich, Simple method for the esterification of carboxylic acids, *Angew. Chem., Int. Ed. Engl.*, 1978, **17**(7), 522–524, DOI: 10.1002/ANIE.197805221.

35 A. Seth, S. Lee, G. Muralikrishnan, E. Garcia, J. Odei, A. H. Mutala, K. Badu and A. K. Badu-Tawiah, Diagnosis on-demand: Field evaluation of microfluidic paper device for the detection of asymptomatic malaria, *Anal. Chem.*, 2025, **97**(22), 11787–11797, DOI: 10.1021/ACS.ANALCHEM.5C01324/SUPPL_FILE/AC5C01324_SI_001.PDF.

36 C. Ge, J. Feng, J. Zhang, K. Hu, D. Wang, L. Zha, X. Hu and R. Li, Aptamer/antibody sandwich method for digital detection of SARS-CoV2 nucleocapsid protein, *Talanta*, 2022, **236**, 122847, DOI: 10.1016/J.TALANTA.2021.122847.

37 Q. Fernandes, V. P. Inchakalody, M. Merhi, S. Mestiri, N. Taib, D. M. A. El-Ellathe, T. Bedhiafi, A. Raza, L. Al-Zaidan, M. O. Mohsen, M. A. Y. Al-Nesf, A. A. Hssain, H. M. Yassine, M. F. Bachmann, S. Uddin and S. Dermime, Emerging COVID-19 variants and their impact on SARS-CoV-2 diagnosis, therapeutics and vaccines, *Ann. Med.*, 2022, **54**(1), 524–540, DOI: 10.1080/07853890.2022.2031274.

38 H. P. Verkerke, G. L. Damhorst, D. S. Graciaa, K. Mclendon, W. O'sick, C. Robichaux, N. Cheedarla, S. Potlapalli,

S. C. Wu, K. R. V. Harrington, A. Webster, C. Kraft, C. A. Rostad, J. J. Waggoner, N. R. Gandhi, J. Guarner, S. C. Auld, A. Neish, J. D. Roback, W. A. Lam, N. S. Shah and S. R. Stowell, Nucleocapsid antigenemia is a marker of acute SARS-CoV-2 infection, *J. Infect. Dis.*, 2022, **226**(9), 1577–1587, DOI: 10.1093/INFDIS/JIAC225.

39 R. McBride, M. van Zyl and B. C. Fielding, The coronavirus nucleocapsid is a multifunctional protein, *Viruses*, 2014, **6**(8), 2991–3018, DOI: 10.3390/V6082991.

40 M. Yang, C. Li, G. Ye, C. Shen, H. Shi, L. Zhong, Y. Tian, M. Zhao, P. Wu, A. Hussain, T. Zhang, H. Yang, J. Yang, Y. Weng, X. Liu, Z. Wang, L. Gan, Q. Zhang, Y. Liu, G. Yang, Y. Huang and Y. Zhao, Aptamers targeting SARS-CoV-2 nucleocapsid protein exhibit potential anti pan-coronavirus activity, *Signal Transduction Targeted Ther.*, 2024, **9**(1), 1–13, DOI: 10.1038/s41392-024-01748-w.

41 D. E. Damon, K. M. Davis, C. R. Moreira, P. Capone, R. Cruttenden and A. K. Badu-Tawiah, Direct biofluid analysis using hydrophobic paper spray mass spectrometry, *Anal. Chem.*, 2016, **88**(3), 1878–1884, DOI: 10.1021/ACS.ANALCHEM.5B04278/SUPPL_FILE/AC5B04278_SI_005.AVI.